Clays and Clay Minerals, Vol. 55, No. 5, 504–518, 2007.

CLAY MINERAL ASSEMBLAGES AND VITRINITE REFLECTANCE IN THE LAGA BASIN (CENTRAL APENNINES, ITALY): WHAT DO THEY RECORD?

LUCA ALDEGA[1,*], FLAVIA BOTTI[2] AND SVEVA CORRADO[1]

[1] Dipartimento di Scienze Geologiche, Università degli Studi 'Roma Tre', L.go S. Leonardo Murialdo, 1, 00146 Roma, Italy
[2] Dipartimento di Scienze della Terra, Università degli Studi di Pisa, Via S. Maria, 53 - 50100 Pisa, Italy

Abstract—Temperature-dependent clay mineral assemblages and vitrinite reflectance data have been used to investigate levels of diagenesis from the Messinian Laga Basin in the Central Apennines developed at the footwall of the Sibillini Mts. and the Gran Sasso Massif. Data are from stratigraphic units forming the main siliciclastic basin fill up to Middle Messinian gypsum-arenites and its pre-orogenic substratum. Specifically, the largest R_om% values and percentages of illite layers in illite-smectie (I-S) are found in the basin depocenter and at the footwall of the main carbonate thrust sheets. Smaller R_om% values, and percentage of illite layers in I-S characterize less subsided sectors surrounding the depocenter.

The X-ray diffraction data were treated using decomposition methods and the peaks identified were rationalized in terms of discrete and/or mixed-layer phases. Complex clay mineral assemblages were found in the Laga Fm. including three sub-populations of illitic material corresponding to authigenic and detrital components. I-S mixed layers record the maximum paleotemperature the Laga Fm. experienced, which is directly related to its burial history. Kübler index (KI) data, however, suggest higher temperatures related to detrital K-micas inherited from the uplift of the Alpine-Apennines chain.

A tentative calculation of paleotemperatures from selected data of organic and inorganic parameters is also proposed and compared with recent sedimentological, stratigraphic and structural data. We conclude that the Laga Basin fill never experienced temperatures of >100−110ºC, generally due to variable sedimentary loading, whereas localized anomalous heating is due to the effect of the tectonic emplacement and subsequent local erosion of the Sibillini and Gran Sasso thrust sheets.

Key Words—Illite, Italy, Kübler Index, Laga Basin, Mixed-layer Clay Minerals, Syn-orogenic Deposits, Thermal Evolution, Vitrinite Reflectance.

INTRODUCTION

Several studies based on the chemical and structural changes in the series smectite−illite-smectite−illite−dioctahedral white mica have been used for assessing the extent of burial diagenesis and the metamorphic grade of sedimentary successions (Hower *et al.*, 1976; Pollastro and Barker, 1986; Leoni *et al.*, 1996; Wang *et al.*, 1996; Carosi *et al.*, 2003). The systematic occurrence of this sequence in very low-grade metamorphic and diagenetic systems coupled with a regular pattern of increasing crystallite size suggests that a 'geothermometer' should exist for rocks forming under low-temperature conditions (Pollastro, 1993). Essene and Peacor (1995) pointed out that although reactions are controlled by many factors (*e.g.* fluid composition, fluid/rock ratio, *etc.*), where such conditions are constrained to be approximately equal, there should be a correlation between reaction progress and temperature.

In general, the Kübler index (KI) is not a precise measure of diagenetic stage because it is dependent on both the quantity and quality of the mixed-layer component of a sample (Weaver and Broekstra, 1984). The contribution of NH_4-bearing phases, K/Na intermediate micas, paragonite, illite-smectite (I-S) mixed layers and other interfering phases significantly influence the shape of illite basal reflections, which may cause a small but systematic increase in the full width at half-maximum intensity (FWHM), possibly leading to petrogenetic misinterpretations (Árkai, 2002). The KI is, however, applicable at the illite stage, when this index becomes a function of the growing size of the coherent scattering domain as illite is transformed into muscovite.

On the contrary, mixed-layer clay minerals, in particular I-S, are good descriptors of diagenesis. The reaction degree, measured as the percentage of illite layers in the I-S and the structural transition from random to ordered mixed layers describes the whole diagenetic zone. It integrates and substitutes KI data for very low-temperature settings.

In siliciclastic sedimentary rocks, detrital grains may occur together with authigenic minerals formed during burial diagenesis. Thus, the region of the diffraction pattern between 5 and 11º2θ may be composed of contributions from both types of components, resulting in complex X-ray diffraction (XRD) patterns (Wang *et al.*, 1995; Gharrabi *et al.*, 1998).

In this paper, we use XRD decomposition methods to describe the features of the various sub-populations forming the illitic assemblages in terms of thermal

* E-mail address of corresponding author:
aldega@uniroma3.it
DOI: 10.1346/CCMN.2007.0550505

indicators. Mixed-layer clay minerals and 'crystallinity' measurements were tested as geothermometers on a turbiditic system, where inherited minerals may hide and overcome diagenetic contributions.

Temperature-dependent clay minerals are therefore integrated with vitrinite reflectance (R_om%; Stach *et al.*, 1982) which is the most reliable technique at recording maximum paleotemperatures and is not affected by retrograde metamorphism (Teichmüller, 1987). Nevertheless R_om% values may be underestimated in areas affected by strong subsidence rates (Heling and Teichmüller, 1974).

In synthesis, different thermal indicators are used and compared to assess their ability to describe the thermal paleoconditions within the studied formation. Their combined use allows us to overcome the 'noise' related to recycling, alteration and high subsidence rates and to propose constraints based on clay mineralogy and organic matter analyses that are useful for reconstructing thermal maturity patterns in the external zones of a fold-and-thrust belt.

MATERIALS

The Laga Basin is located to the East of the Sibillini Mts. and to the North of the Gran Sasso Range that represent two of the main Meso-Cenozoic carbonate backbones of the Central Apennines (Figures 1 and 2). To the East the basin is limited by the N−S structural relief of Montagnone-Montagna dei Fiori. Since the Lower Messinian, this basin has exhibited features consistent with either a foreland basin or a wedge-top basin and the siliciclastics of the Laga Fm. filled it up (Centamore *et al.*, 1991; Artoni, 2003; Moscatelli *et al.*, 2004; Manzi *et al.*, 2005; Bigi *et al.*, 2006). These deposits unconformably overlie the pre-orogenic substratum of the Umbria-Marche pelagic carbonate succession which records a complex tectono-stratigraphic evolution during Neogene times (Moscatelli *et al.*, 2004).

We focused sampling on the Laga Fm. to the west of the Montagnone-Montagna dei Fiori alignment where facies architecture, subsidence amounts, and tectonic loadings (now eroded) vary considerably along both strike and dip of the fold-and-thrust belt (Figures 1 and 2). The Laga Fm. is classically subdivided into three members (Centamore *et al.*, 1991): pre-evaporitic (Lower Messinian), evaporitic (Middle Messinian) and post-evaporitic (Upper Messinian). Our investigation mainly refers to the pre-evaporitic member from which 36 samples were collected for vitrinite reflectance and XRD analyses. This member consists of various lithology associations. From bottom up, thick sandstone strata separated by thin shale laminae (arenaceous association) grade upward into thinner arenaceous-pelitic horizons (arenaceous-pelitic association) and more abundant clay-rich sediments in which thick arenaceous layers are interbedded (pelitic-arenaceous association). This succession generally evolves into hemipelagic deposits with very thin intercalations of fine-grained siltites and sandstones (pelitic association).

Two additional samples pertain to the gypsum arenites of the evaporitic member of the Laga Fm.

Subordinately, the pre-orogenic succession which represents the marly-calcareous substratum of the basin was sampled at eight sites along the structural culminations surrounding the basin (*i.e.* the Montagna dei Fiori area). These deposits are characterized by various lithostratigraphic units such as marly limestones containing the organic-rich Bonarelli level (from the Scaglia Bianca Fm.), calcareous marls (from Rosso Ammonitico Fm.), and marls (from Marne a Fucoidi and Marne con Cerrogna Fms).

METHODS

Clay mineralogy

The XRD analyses were performed using a Scintag X_1 XRD system (CuKα radiation, solid-state detector, spinning sample) at 40 kV and 45 mA. Randomly-oriented whole-rock powders were run in the 2−70º2θ interval with a step size of 0.05º2θ and a counting time of 3 s per step. Oriented air-dried (AD) samples were scanned from 1 to 48º2θ with a step size of 0.05º2θ and a count time of 4 s per step. The presence of expandable clay minerals was determined for samples treated with ethylene glycol at room temperature for 24 h. Ethylene glycol (EG)-solvated samples were scanned at the same conditions as air-dried aggregates with a scanning interval of 1−30º2θ. The <2 μm grain-size fraction was separated by centrifuging, and oriented slides were prepared by the pipette-on-slide method (Moore and Reynolds, 1997), keeping the specimen thickness as constant as possible, with at least 3 mg of clay per cm^2 of glass slide (Kisch, 1991).

Expandability measurements for both I-S and chlorite-smectite (C-S) mixed-layer minerals were determined according to Moore and Reynolds (1997) using the ºΔ2θ method after decomposing the composite peaks between 9−10º2θ and 16−17º2θ for I-S and between 10−12.3º2θ and 25−26º2θ for C-S using a split Pearson VII function.

'Illite crystallinity' measurements (KI) are made by first subtracting the background from the raw data, and then applying a profile-fitting method (Lanson, 1997). From the fitted data, the crystallinity was determined by the FWHM parameter of the program. Half-peak widths were calibrated using Warr and Rice's standards (1994).

The 10 Å asymmetric illitic multiphase peak was fitted using the Scintag X_1 software. Peak shape decomposition was performed on both AD and EG preparations using split Pearson VII functions. The peaks identified were rationalized in terms of specific discrete or mixed-layer I-S and/or C-S phases (Lanson, 1997).

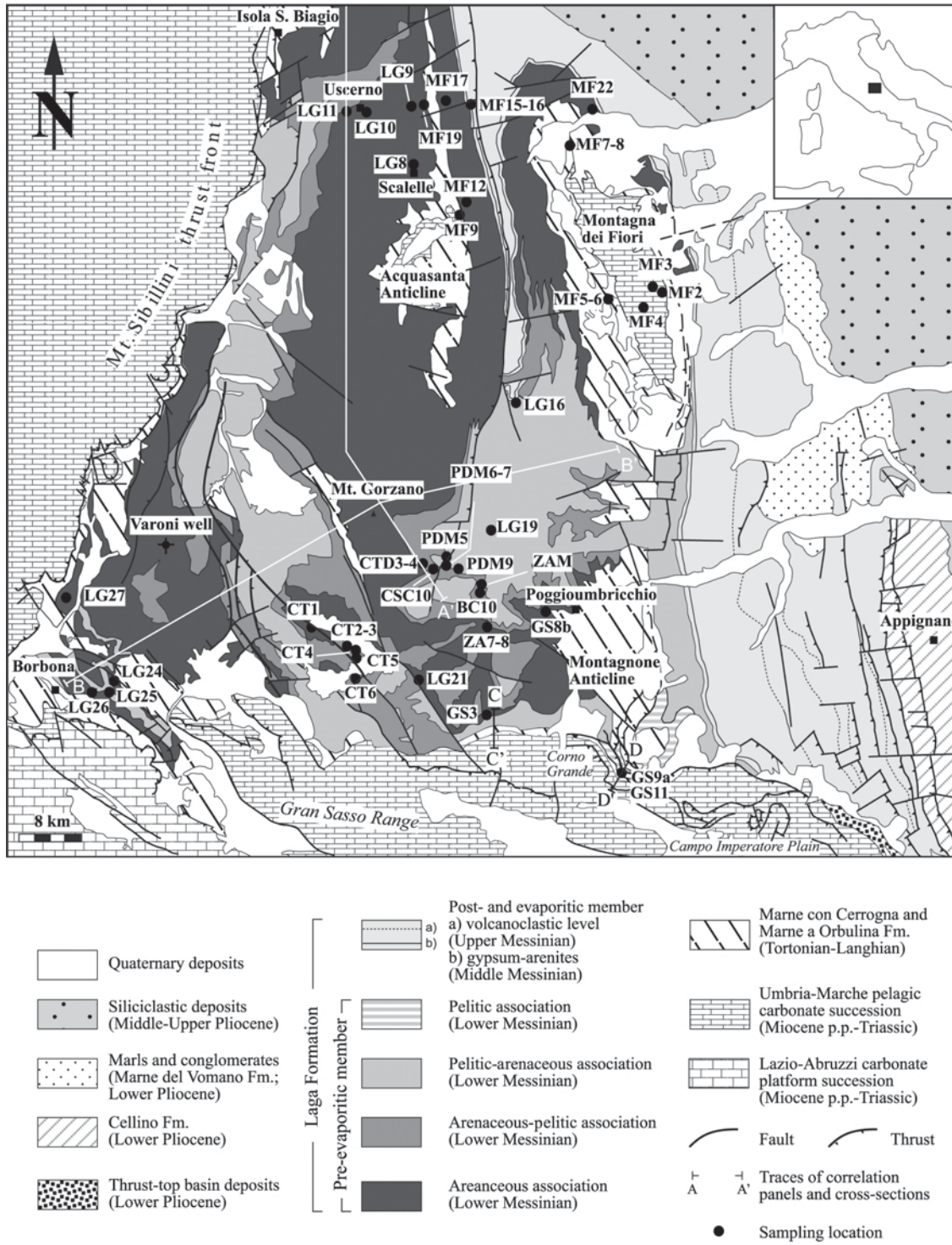

Figure 1. Geological sketch map of the Laga Basin with sampling sites, redrawn and modified after Centamore *et al.* (1991).

Peaks relatively close in position were selected for clay mineral quantitative analysis of the <2 μm (equivalent spherical diameter) in order to minimize the angle-dependent intensity effect. Integrated peak areas were transformed into mineral concentrations by using mineral intensity factors as a calibration constant (see Moore and Reynolds, 1997, for a review).

Non-clay minerals that were recognized in the <2 μm grain-size fraction were not included in the quantitative analysis of the oriented aggregates, thus the data given

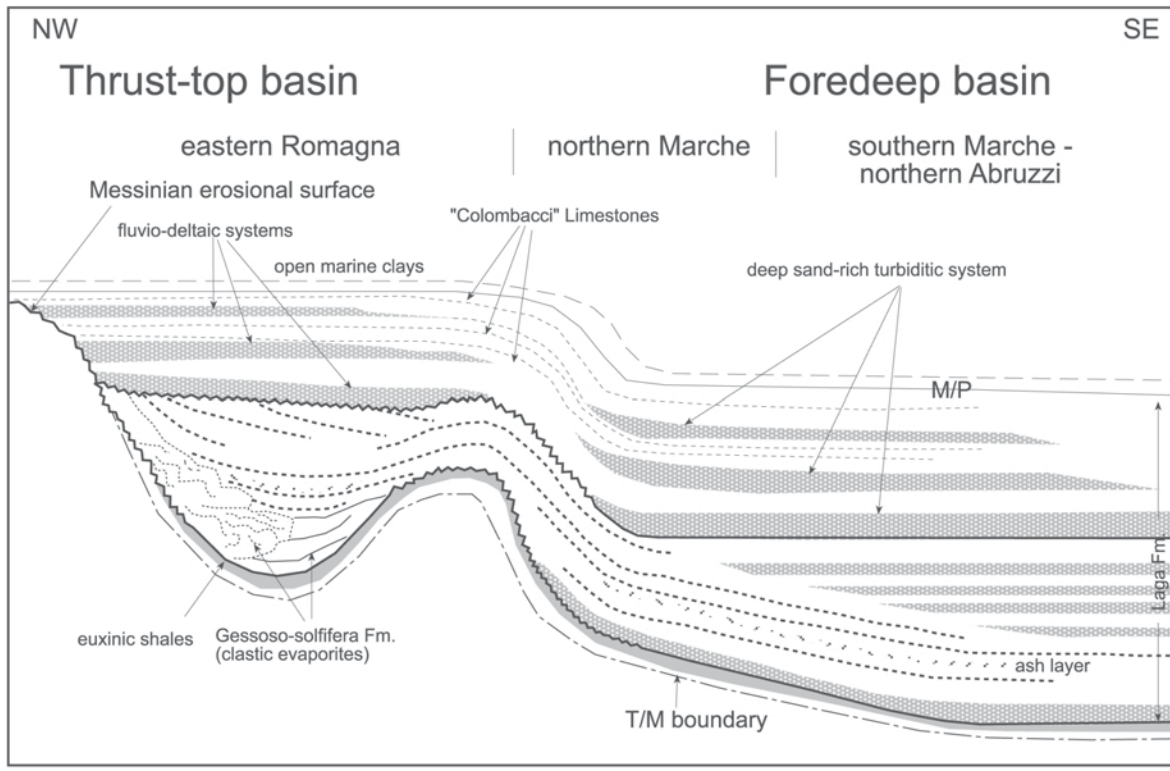

Figure 2. Schematic geological setting of the northern Apennines during the late Messinian (Pliocene base as datum plane) and relationships between basinal settings (eastern Romagna-northern Marche basins and Laga Basin). T/M: Tortonian/Messinian boundary; M/P: Messinian/Pliocene boundary (after Manzi *et al.*, 2005, redrawn and modified).

refer to the phyllosilicate group only. The amounts of clay minerals were not recalculated into percentages of bulk rock, but represent the content of the <2 μm grain-size fraction.

Vitrinite reflectance

Mean random vitrinite reflectance (R_om%) was measured on whole-rock samples rich in coaly particles collected from sandstone, siltstone and clayey lithologies. Samples were first mounted in epoxy resin and polished. Vitrinite reflectance analyses were then performed on randomly oriented grains using a Zeiss Axioplan microscope and conventional microphotometric methods, under oil immersion (n = 1.518) in reflected monochromatic non-polarized light (λ = 526 nm). Reflectance standards (R_om% = 0.418% and 0.580%) were used for calibration. In most cases a population of a few tens of readings per sample were made on fragments only slightly fractured and/or altered (Borrego *et al*., 2006).

RESULTS

Mineralogical data

Pre-orogenic succession. Analyzed marl samples belong to the Marne con Cerrogna, Marne a Fucoidi and Rosso Ammonitico Fms (Table 1). An example of a typical XRD pattern of the pre-orogenic succession is shown in Figure 3a. Excluding the 14 Å chlorite peak, two elementary peaks in the AD specimen (Figure 3b) are required for a good fit of the diffraction pattern between 5 and 11°2θ. A peak at high 2θ (~8.85°2θ) is attributed to discrete illite, whereas a wider peak at lower 2θ (~6.35°2θ) is attributed to R0 I-S mixed layers. In the EG case a third peak is added corresponding to I001-S002 mixed layers (Figure 3c).

The Marne con Cerrogna Fm. is characterized by illite, I-S, chlorite, kaolinite and non-clay minerals such as quartz, calcite and albite. I-S are R0 structures in which the illite content is in the range 48−50%. The KI values range from 0.89 to 1.01°Δ2θ and from 0.94 to 1.08°Δ2θ in the EG and AD diffraction patterns, respectively (Table 1).

The Marne a Fucoidi Fm. is mainly composed of illite and I-S in which the smectite component is dominant. The calculated percentage of illite layers in I-S is 40%. The KI values are 1.01 and 1.08°Δ2θ for the EG and AD oriented mounts, respectively.

A slightly different mineral assemblage characterizes the Rosso Ammonitico Fm. Illite, I-S, chlorite and C-S mixed layers are the recognized clay minerals. Kaolinite is absent. I-S corresponds to short-range ordered structures with an illitic content of 64%. The Rosso

Table 1. Organic matter maturity and clay mineralogy data.

Sample	Lithology	R_om%±sd (*n.* meas.)	%I in I-S (R parameter)	%C in C-S	KI (°Δ2θ) AD	KI (°Δ2θ) EG	XRD analysis <2 μm	XRD analysis Whole rock
Gypsum arenites (Laga Fm.)								
MF16	shale	0.308±0.039 (100)	–	–	–	–	–	–
MF15	sandstone	0.326±0.051 (102)	–	–	–	–	–	–
Pelitic association (Laga Fm.)								
GS9a	shale	0.459±0.064 (28)	–	–	–	–	–	$Qtz_8Kfs_1Ab_{13}Ph_{78}$
GS11	shale	0.473±0.036 (290)	–	–	–	–	–	–
Pelitic-arenaceous association (Laga Fm.)								
LG19	shale	0.470±0.072 (73)	52 (R0)	–	0.68	0.59	$I_{60}I\text{-}S_{18}K_5Ch_{17}$	$Qtz_8Cal_{22}Ab_9Ph_{50}Dol_9Py_2$
PDM5	shale	0.418±0.113 (12)	51 (R0)	–	0.54	0.52	$I_{63}I\text{-}S_6K_9Ch_{22}$	$Qtz_8Cal_{20}Kfs_1Ab_4Ph_{65}Py_2$
PDM6	shale	0.356±0.136 (10)	52 (R0)	–	0.60	0.54	$I_{62}I\text{-}S_7K_7Ch_{24}$	$Qtz_9Cal_2Kfs_1Ab_{13}Ph_{75}$
LG16	sandstone	0.248±0.034 (42)	50 (R0)	62	0.66	0.65	$I_{40}I\text{-}S_{14}C\text{-}S_{38}K_3Ch_5$	$Qtz_{13}Cal_{10}Kfs_2Ab_{29}Ph_{39}Dol_6Py_1$
LG25	sandstone	0.450±0.029 (59)	50 (R0)	65	0.53	0.50	$I_{52}I\text{-}S_9C\text{-}S_{15}Ch_{24}$	$Qtz_{21}Cal_{14}Kfs_2Ab_{34}Ph_{18}Dol_{11}$
GS8b	sandstone	0.414±0.034 (15)	–	–	–	–	–	$Qtz_8Cal_{17}Ab_8Ph_{59}Dol_6Py_2$
PDM7	sandstone	–	50 (R0)	62	0.52	0.51	$I_{50}I\text{-}S_5C\text{-}S_{20}K_8Ch_{17}$	$Qtz_{22}Cal_9Kfs_1Ab_{33}Ph_{32}Dol_3$
PDM9	sandstone	–	50 (R0)	65	0.63	0.48	$I_{53}I\text{-}S_9C\text{-}S_{15}K_7Ch_{16}$	$Qtz_{25}Cal_{15}Kfs_1Ab_{33}Ph_{23}Dol_3$
Arenaceous-pelitic association (Laga Fm.)								
CT3	shale	–	50 (R0)	–	0.57	0.54	$I_{70}I\text{-}S_7Ch_{23}$	–
CT4	shale	–	74 (R1)	–	0.88	0.71	$I_{56}I\text{-}S_{15}K_8Ch_{21}$	–
CSC10	shale	0.579±0.138 (52)	76 (R1)	–	0.70	0.69	$I_{56}I\text{-}S_{25}K_6Ch_{13}$	$Qtz_8Cal_{18}Ab_5Ph_{59}Dol_6Py_4$
BC10	shale	0.313±0.087 (19)	50–70 (R0-R1)	62	0.99	0.84	$I_{60}I\text{-}S_{24}C\text{-}S_3K_3Ch_{10}$	$Qtz_9Cal_{16}Ab_8Ph_{63}Dol_4$
CT2	sandstone	–	–	63	0.54	0.54	$I_{27}C\text{-}S_{33}K_{16}Ch_{24}$	$Qtz_{24}Cal_{15}Kfs_2Ab_{42}Ph_{16}Dol_1$
CT5	sandstone	0.419±0.103 (13)	49–73 (R0-R1)	–	0.83	0.64	$I_{50}I\text{-}S_{20}K_{12}Ch_{18}$	$Qtz_{17}Cal_{25}Kfs_1Ab_{18}Ph_{34}Dol_5$
CT6	sandstone	0.510±0.040 (9)	73 (R1)	–	0.72	0.64	$I_{37}I\text{-}S_{12}K_6Ch_{45}$	$Qtz_{19}Cal_{14}Kfs_1Ab_{38}Ph_{22}Dol_6$
CTD4	sandstone	–	50–70 (R0-R1)	66	0.53	0.49	$I_{38}I\text{-}S_6C\text{-}S_{15}K_{16}Ch_{25}$	$Qtz_{22}Cal_{12}Kfs_2Ab_{32}Ph_{26}Dol_6$
CTD3	sandstone	0.488±0.037 (30)	50−70 (R0−R1)	65	0.53	0.49	$I_{36}I\text{-}S_7C\text{-}S_{14}K_{14}Ch_{29}$	$Qtz_{23}Cal_{15}Kfs_2Ab_{33}Ph_{20}Dol_7$
ZAM	sandstone	0.443±0.048 (36)	–	–	–	–	–	–
Arenaceous association (Laga Fm.)								
ZA7	shale	–	66 (R1)	70	0.68	0.51	$I_{59}I\text{-}S_{16}C\text{-}S_7K_5Ch_{13}$	–
ZA8	shale	0.368±0.039 (4)	65 (R1)	70	0.66	0.59	$I_{56}I\text{-}S_{10}C\text{-}S_7K_8Ch_{19}$	$Qtz_{21}Cal_{25}Kfs_1Ab_{29}Ph_{21}Dol_3$
LG11	sandstone	0.385±0.027 (40)	–	–	–	–	–	$Qtz_{22}Cal_2Kfs_1Ab_{50}Ph_{18}Dol_5Gy_2$
LG21	sandstone	0.536±0.085 (24)	60 (R1)	57	0.66	0.58	$I_{44}I\text{-}S_{15}C\text{-}S_5K_9Ch_{27}$	$Qtz_{23}Cal_7Kfs_1Ab_{37}Ph_{26}Dol_6$
LG24	sandstone	–	–	53	0.39	0.34	$I_{30}C\text{-}S_{60}Ch_{10}$	$Qtz_{29}Cal_{19}Kfs_2Ab_{35}Ph_{14}Dol_1$
LG26	sandstone	0.474±0.036 (99)	–	–	–	–	–	–
LG27	sandstone	0.365±0.060 (25)	–	40	0.39	0.36	$I_{46}C\text{-}S_{40}Ch_{14}$	$Qtz_{21}Cal_{14}Kfs_3Ab_{43}Ph_{14}Dol_2$
MF12	sandstone	0.332±0.099 (44)	–	–	–	–	–	–
MF17	sandstone	0.376±0.054 (11)	–	–	–	–	–	–
MF19	sandstone	0.289±0.047 (102)	–	–	–	–	–	–
MF22	sandstone	0.382±0.057 (9)	–	–	–	–	–	–
GS3	sandstone	0.378±0.031 (20)	–	–	–	–	–	$Qtz_7Cal_{22}Ab_3Ph_{60}Dol_6Py_2$
CT1	sandstone	0.370±0.052 (35)	–	63	0.43	0.43	$I_{28}C\text{-}S_{29}K_{10}Ch_{33}$	$Qtz_{29}Kfs_1Ab_{42}Ph_{28}$

LG8	sandstone	0.398±0.053 (34)	60 (R1)	62	0.68	0.59	$I_{55}I\text{-}S_{24}C\text{-}S_3K_5Ch_{13}$	$Qtz_{23}Cal_3Kfs_1Ab_{16}Ph_{40}Dol_{17}$
LG10	coal	0.383±0.056 (100)	–	–	–	–	–	–
LG9	coal	0.367±0.028 (31)	–	–	–	–	–	–
Pre-orogenic succession [Marne con Cerrogna (mc), Scaglia Bianca (sb), Marne a Fucoidi (mf), Rosso Ammonitico (ra)]								
MF9	marl (mc)	–	50 (R0)	–	1.03	0.98	$I_{50}I\text{-}S_{16}K_{14}Ch_{20}$	–
MF7	marl (mc)	–	50 (R0)	–	1.07	1.01	$I_{55}I\text{-}S_{29}K_7Ch_9$	–
MF8	marl (mc)	–	50 (R0)	–	0.99	0.91	$I_{49}I\text{-}S_{13}K_{12}Ch_{26}$	–
MF5	marl (mc)	–	50 (R0)	–	1.08	1.01	$I_{61}I\text{-}S_{24}K_7Ch_8$	–
MF6	marl (mc)	–	48 (R0)	–	0.94	0.89	$I_{55}I\text{-}S_{24}K_8Ch_{13}$	–
MF2	coal (sb)	0.419±0.084 (46)	–	–	–	–	–	–
MF3	marl (mf)	–	40 (R0)	–	1.08	1.01	$I_{59}I\text{-}S_{41}$	–
MF4	marl (ra)	–	64 (R1)	65	1.11	1.03	$I_{66}I\text{-}S_{29}C\text{-}S_3Ch_2$	–

For the <2 μm grain-size fraction: Sm = smectite; I = illite; I-S = illite-smectite mixed layers; K = kaolinite; Ch = chlorite
For the whole-rock samples: Qtz = quartz; Cal = calcite; Ph = phyllosilicates; Ab = albite; Kfs = K-feldspar; Dol = dolomite; Py = pyrite; Gy = gypsum

Ammonitico Fm. has KI values of ~1.0−1.1°Δ2θ, similar to the overlying deposits.

Syn-orogenic succession (Laga Fm.). Analysis of randomly-oriented whole-rock powder patterns shows that shales and sandstones of the Laga Fm. are composed essentially of quartz, albite, dolomite, calcite, small amounts of K-feldspar and clay minerals. Pyrite, gypsum and gismondine are also observed in a few samples as minor phases (Table 1).

The <2 μm grain-size fraction in shales and sandstones is composed mostly of illite, I-S, C-S, kaolinite and chlorite and subordinate non-clay minerals such as quartz, albite, calcite and gismondine. The C-S is mainly restricted to sandstones and its mean composition is C(62%)-S(38%). The I-S from sandstone contains less illite than does I-S from shale in each lithology association. This difference in the amount of illite in I-S of sandstone *vs.* shale can be explained by considering the possible origin of I-S in these two lithologies (Pollastro and Barker, 1986). The I-S in sandstones is largely an authigenic matrix that reflects the physical and chemical conditions existing in the porous rock at the time of its formation. In shale, I-S is mainly detrital and is from different sources including rocks that could have undergone more extensive diagenetic reactions.

The pelitic-arenaceous lithology association shows mixed-layer I-S with random interstratification in which the illitic content is ~50−52%.

Ordered and disordered I-S were identified in the underlying arenaceous-pelitic lithology association (Figure 4a). Three distinct sub-populations of illitic assemblages have been identified by using a profile-fitting method (Lanson, 1997). Figure 4b shows that four elementary peaks were required to model the experimental diffraction area in the AD patterns.

These peaks correspond to discrete illite which is unaffected by EG solvation, ordered I-S with smectite layers that do not exceed 25%, disordered I-S with smectite content in the 50−52% range and chlorite. In the EG patterns (Figure 4c), two additional peaks between 9 and 11°2θ are considered to correspond to the I001-S002 reflections of R1 and R0 mixed-layer clay minerals. When C-S mixed layers were identified, the decomposition of the low-angle diffraction region requires an additional peak.

Only R1 I-S were recognized in the arenaceous lithology association.

The FWHM expressed as Kübler index is variable (Figure 5) ranging from 0.39 to ~1.0°Δ2θ in the AD specimen and from 0.34 to 0.84°Δ2θ in the EG-oriented mounts.

Vitrinite reflectance

Analyses in reflected light provided reliable R_om% values for 30 samples in terms of the number of analyzed fragments and measurement distribution (Table 1). Data

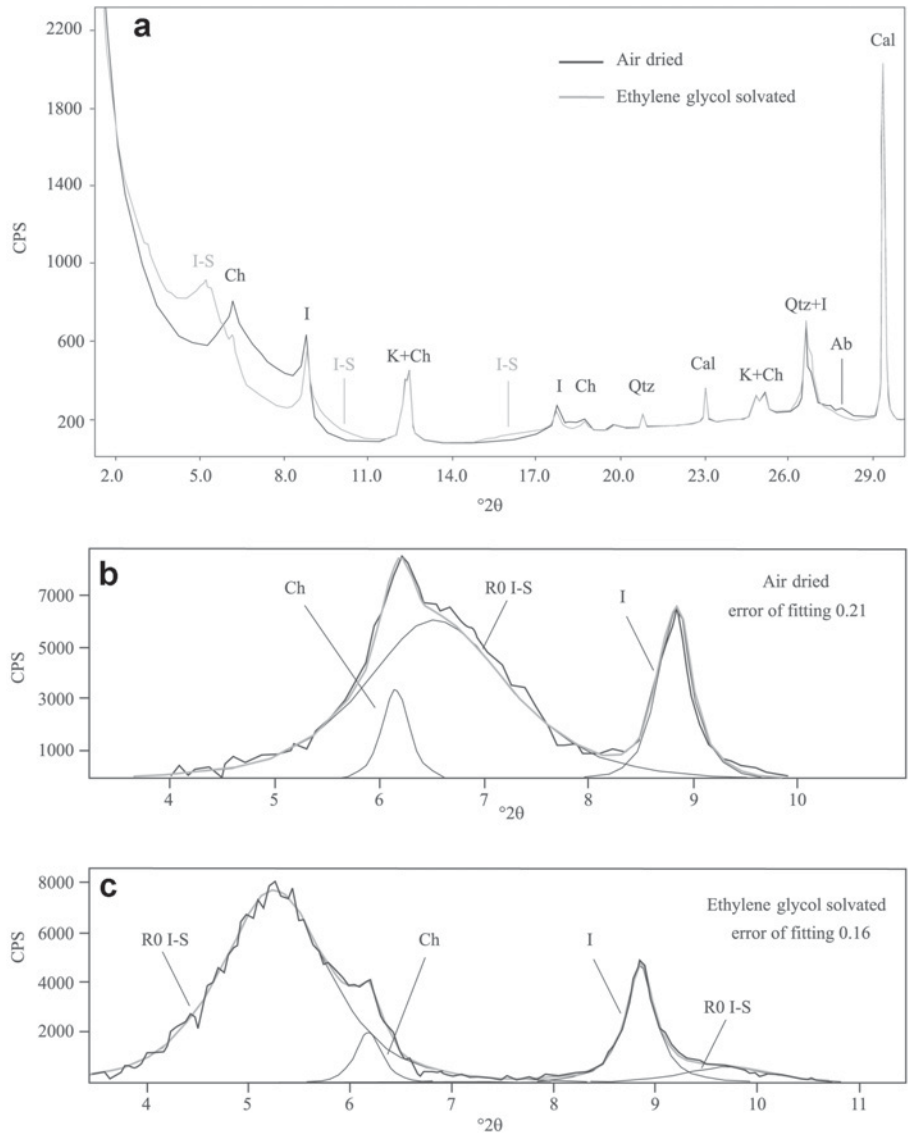

Figure 3. (a) EG and AD diffraction patterns for the MF8 sample (pre-orogenic succession) in the <2 μm grain-size fraction. Ch = chlorite, I-S = illite-smectite, I = illite, K = kaolinite, Qtz = quartz, Cal = calcite, Ab = albite. Parts b and c show the complex XRD bands decomposed using the Scintag X1 software with split Pearson VII functions. CuKα radiation.

generally show one main cluster identifying the possible indigenous population of vitrinite-humite macerals (examples from different lithology associations in Figure 6). The R_om% data indicate immature to early mature stages of hydrocarbon generation with slight variations within the study area.

In the pre-orogenic succession, only one sample provided reliable results from the Bonarelli level found almost at the top of the Scaglia Bianca Fm. Numerous measurements on thermally altered fragments of higher plants indicate a low thermal maturity with R_om% values of ~0.42%. These components generally co-exist with prevalent fusinite, and both are diluted in abundant amorphous organic matter alternating with pyrite bands. Thus R_om% values might be underestimated (Price and Barker, 1985).

In the Laga Fm. the organic matter dispersed in sediments is generally abundant, homogeneous and mainly made up of well preserved macerals. They belong mainly to the huminite-vitrinite group, with predominant collotelinite and telinite fragments, and subordinate amounts of inertinite group macerals (*i.e.* fusinite). Pyrite either finely dispersed or in small globular aggregates is locally present along the rims of huminite-vitrinite macerals.

Data from the Laga Fm. indicate that the pre-evaporitic member (Lower Messinian) shows a range of R_om% values between 0.29 and 0.58% indicating immature to early mature stages, whereas the evaporitic member is richer in vitrinite fragments and R_om% indicates the immature stage that corresponds to ~0.32%.

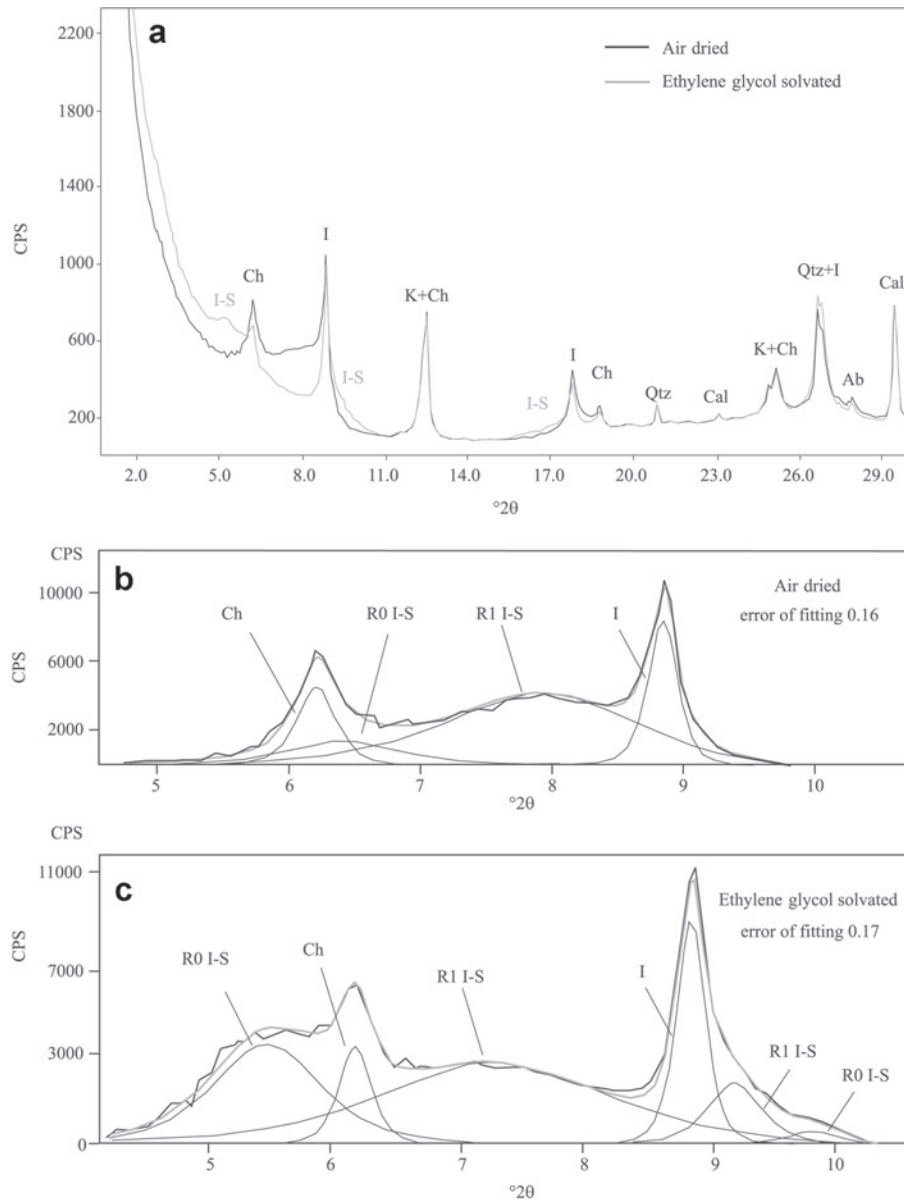

Figure 4. (a) EG and AD diffraction patterns for the CT5 sample (syn-orogenic succession) in the <2 μm grain-size fraction. Ch = chlorite, I-S = illite-smectite, I = illite, K = kaolinite, Qtz = quartz, Cal = calcite, Ab = albite. Parts b and c show the complex XRD bands decomposed using the Scintag X1 software with split Pearson VII functions. CuKα radiation.

DISCUSSION

In the external zones of fold-and-thrust belts, where levels of thermal evolution are generally low, it is difficult to discriminate between various contributions to thermal maturity due to either tectonic or sedimentary burial. This is particularly true for sedimentary successions deposited in basins characterized by highly variable subsidence rates such as syn-orogenic basins.

Furthermore, illite crystals in siliciclastic sediments are heterogeneous assemblages of detrital material from various source rocks, and, at paleotemperatures >70ºC (Merriman and Kemp, 1996), of superimposed diagenetic modifications of this sediment. Only authigenic (diagenetic) rather than detrital phases should be used to estimate paleotemperatures and to constrain the burial history of folded and thrust sedimentary successions.

To relate KI data and the percentage of illite layers in I-S to maximum paleotemperatures and to the other organic thermal indicators, we adopted the basin maturity chart proposed by Merriman and Frey (1999). The transition from the Early Diagenetic Zone to the Late Diagenetic Zone is marked by 60–80% illite in I-S, KI values of ~1.0ºΔ2θ, R_om = 0.5% and is placed at a temperature of 100ºC. At this critical reaction temperature, a major change from random to short-range ordered

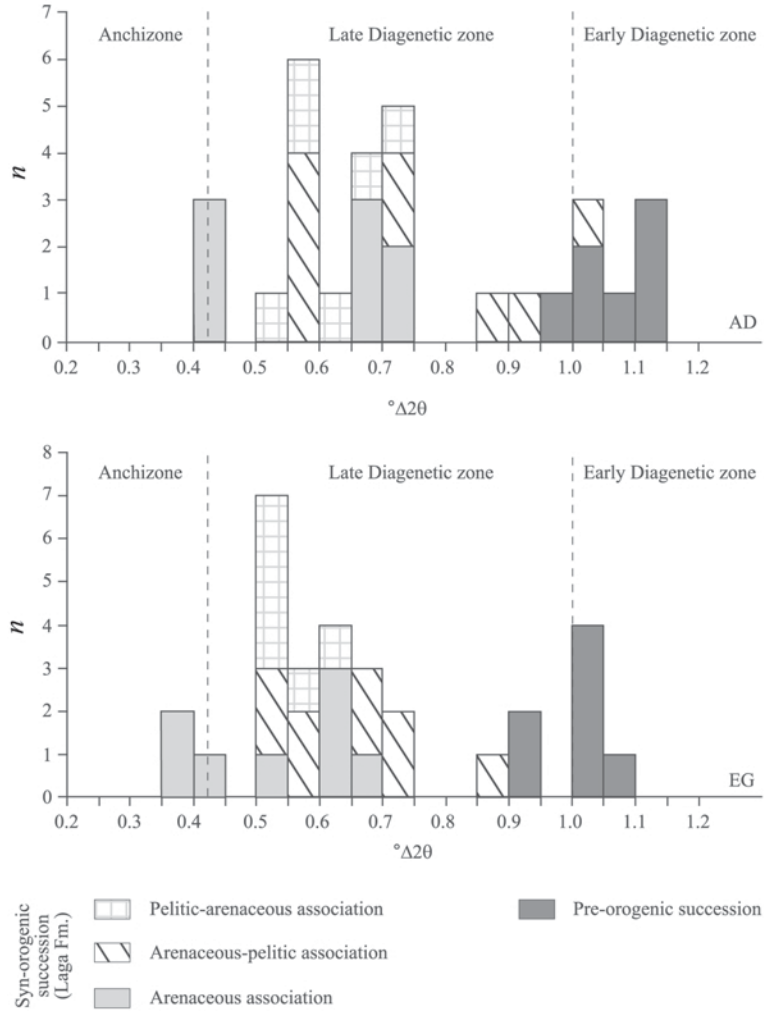

Figure 5. Frequency histograms of KI data for AD and EG specimens. *n* = number of samples examined.

I-S has been documented by many authors (*i.e.* Hoffman and Hower, 1979; Środoń, 1999).

Mixed-layer I-S clay minerals become more illitic (up to 95%) within late diagenesis and long-range ordering appears at temperatures of 170−180ºC (Hoffman and Hower, 1979; Pollastro, 1993). The transition to the anchizone (~200ºC) is indexed at KI of 0.42ºΔ2θ, associated with vitrinite reflectance values of 2.0% and further reduction in smectite content of I-S. KI values of 0.25ºΔ2θ and vitrinite reflectance measurements greater than 4% characterize the transition to the epizone and low-grade metamorphism which occurs at ~300ºC (Bucher and Frey, 1994).

This chart does not consider the reaction progress of trioctahedral phyllosilicates which can be found associated in deeply buried and largely undeformed basinal sedimentary sequences. Usually, C-S mixed layers first appear in diagenesis at temperatures of 60−160ºC (Hillier, 1993; Środoń, 1999).

Furthermore, to convert vitrinite reflectance data properly into paleotemperatures, we complemented Merriman and Frey's chart, which lacks resolution for

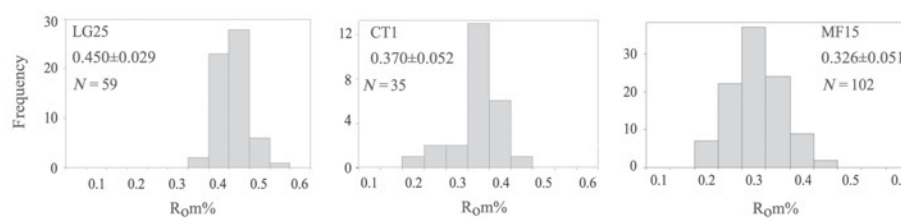

Figure 6. Examples of frequency histograms of R_om% data for the Laga Fm. specimens.

R_om values of <0.5%, using the equation proposed by Barker and Pawlewicz (1994). It was developed as an empirical calibration based on the assumption that temperature has the dominant influence in increasing R_om%, and the effect of heating time is usually on the order of the 'noise' in the experimental determination of R_om% values (Price, 1983; Barker, 1989, 1996). This is due to the fact that sampling strategy and outcrop conditions did not offer the opportunity to build refined time-temperature modeling based on both geological and organic maturity inputs (Allen and Allen, 1993).

The complex clay mineral assemblages found in the Laga Fm. include three sub-populations of illitic material corresponding to authigenic and detrital components. Which of these sub-populations can be used for assessing the thermal evolution of the Laga Basin?

The mixed-layer I-S phases identified are random and short-range ordered I-S with the percentage of illite layers ranging from 50 to 76% in Laga samples (Table 1).

R1 I-S are primarily grouped in a small area to the south of Gorzano Mt. (Figure 1) which is part of the depocenter of the basin identified on the base of field and seismic data (Bigi and Casero, 2006). Moving to the West and the North a progressively less severe thermal evolution is recorded; close to the depocenter, both R0 and R1 I-S were recognized in the same samples, whereas only random stacked mixed-layer clay minerals were found further away.

Both random and short-range ordered I-S are interpreted as the authigenic phases that were formed during burial diagenesis since Messinian times. They suggest early diagenetic conditions and associated paleotemperatures between 60 and 110ºC (Figure 7; Hoffman and Hower, 1979; Merriman and Frey, 1999; Środoń, 1999). This is in agreement with the presence of C-S mixed layers in most samples of which the first appearance in diagenesis is generally associated with temperatures of 60−160ºC (Figure 7; Hillier, 1993).

Decomposed 10 Å peaks of the arenaceous association of the Laga Fm. are considerably narrow (Figure 5 and Table 1). Calibrated KI values (<0.40º$\Delta 2\theta$) record anchizone conditions and a temperature of at least 200ºC

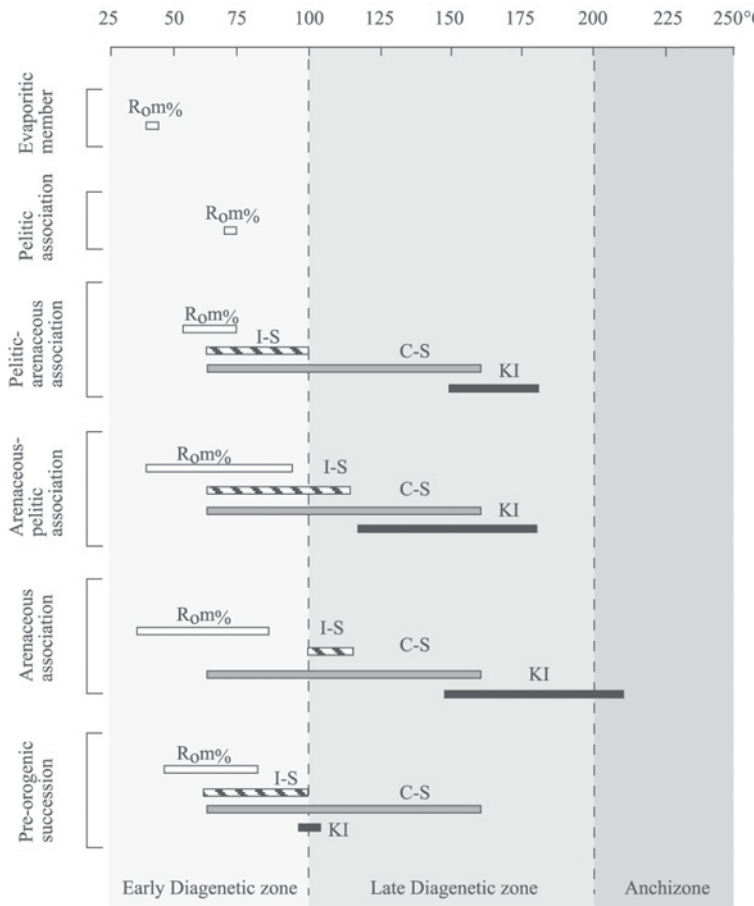

Figure 7. Temperature ranges derived from organic and inorganic thermal parameters. Note that KI-derived temperatures for the Laga Fm. do not match other ranges because the 10 Å phases come from either metamorphic or late diagenetic rocks. R_om%-derived temperatures for the Laga Fm. are generally lower than those calculated from mixed-layer clay minerals (see text for explanation). They refer to minimum and maximum R_om%-derived values without considering the standard deviation of each sample.

(Merriman and Frey, 1999). We interpreted these peaks as the signature of detrital white micas inherited from the uplift of the Alpine chain. These micas probably avoided any significant chemical weathering during their short transport history and record conditions inherited from the past, generally of higher temperature, not directly related to the burial history of the Laga Fm. Instead, KI values between 0.52 and 0.72°Δ2θ, also present in the other lithology associations, fall in late diagenesis (Figure 5, Table 1). This means that the detrital fraction of the Laga Fm. also contains 10 Å phases originating from diagenetic rocks eroded in the source areas. This is in agreement with petrographic data by Corda and Morelli (1996) and Valloni *et al.* (2002) which show a compositional evolution of lithic fragments (from metamorphic to sedimentary) in the Laga Fm. related to changes in the supply area.

Thus, KI data cannot be used for the reconstruction of the thermal history of the Laga Basin but provide information on provenance and thermal condition of the source rock.

Nevertheless, we cannot rule out the possibility that temperatures derived from KI data could be overestimated using the adopted calibration. Kisch *et al.* (2004) suggest that Warr and Rice's scale boundaries (1994) appear not to be equivalent to the original Kübler scale and the boundary values of the anchizone should be shifted towards higher °Δ2θ values (see also Leoni, 2001).

In the pre-orogenic succession, KI-derived temperatures approach those calculated from I-S compositions (Figure 7). Both parameters are consistent with an early and late diagenesis boundary suggesting a maximum temperature not exceeding 100ºC. The agreement between temperature-dependent clay mineral parameters and the slow sedimentation rates allow us to state that detrital contributions may have been unimportant for this succession.

Paleotemperatures derived from Barker and Pawlewicz's equation (1994) for the pre-evaporitic Laga Fm. are always <100ºC with a mean value of <60ºC irrespective of the stratigraphic position within the pre-evaporitic basin (Figure 7). Lowest values are recorded for the evaporitic member with maximum paleotemperatures between 40 and 45ºC. On the other hand, data from the pre-orogenic substratum are very scarce and indicate paleotemperatures of ~65ºC, probably slightly underestimated because of the presence of amorphous organic matter.

Recent sedimentological work on basin architecture has been performed in the area (Milli *et al.*, 2004, 2006, and references therein) through detailed analyses of several field logs that allowed the thickness distribution of the Laga Fm. between the pre-orogenic substratum and the gypsum level within the evaporitic member to the West of the N-S Montagnone-Montagna dei Fiori alignment to be documented. This basin fill is organized into three main sequences (Figure 8). In this framework, among Gorzano Mt., Vomano R. and the Poggioumbricchio area, the main depocenter of the basin developed in Lower Messinian times, whereas thickness tends to decrease to the North moving towards Uscerno village, to the West towards the Sibillini thrust front and to the East towards the N–S structural high where onlap geometries of the Laga Fm. can be observed in the Poggioumbricchio area (Artoni, 2003; Milli *et al.*, 2004). This distribution allowed us to interpret our data in light of the tectono-sedimentary evolution of the basin during Lower–Middle Messinian times.

In Figure 8, we compare calculated maximum burial and the stratigraphic thickness of the Laga Fm. between the pre-orogenic substratum and the gypsum level. Loads were calculated from paleotemperatures assuming a pre-erosional geothermal gradient of 22ºC/km and a surface temperature of 10ºC, based on values for similar successions and tectonic context (Zattin *et al.*, 2002).

Estimated burials based on clay mineralogy in the Lower Messinian depocenter located between Gorzano Mt. and Vomano R. range from ~2.2 to 4.0 km and generally agree with measured or extrapolated stratigraphic sections by Milli *et al.* (2006). The R_om% values generally underestimate burial depths which can be ascribed to very rapid subsidence and failure of the coalification to keep pace with the increase in temperature (Heling and Teichmüller, 1974).

Moving to the North in the Uscerno area, the available R_om% data indicate a maximum burial of ~1.3–1.6 km in a general agreement with measured stratigraphic thicknesses of ~1.4–2.5 km.

Local anomalies are recorded at the footwall of regional Sibillini Mts. and Gran Sasso thrust sheets. At the footwall of the Sibillini thrust sheet, in the Borbona area, stratigraphic thicknesses proposed by Milli *et al.* (2006) are between 1 and 1.5 km whereas maximum burial depths of >2 km were estimated based on either C-S and random I-S coexistence or unoxidized R_om% values between 0.45 and 0.50%. Thus it seems realistic that this area subdued the thermal imprinting of the presently eroded Sibillini thrust sheet, the emplacement of which occurred in the Lower Pliocene (Parotto and Praturlon, 1975; Centamore *et al.*, 1991).

In front of the Gran Sasso structure, no complete reconstruction of the sedimentary thicknesses of the Laga Fm. is available. Nevertheless, we observe that to the North of Corvo Mt. (western Gran Sasso front; C–C' in Figure 9), the R_om% values for the arenaceous lithology association indicate the immature stage of hydrocarbon generation with maximum calculated burials of <1.5 km, while to the North of the Corno Grande thrust fault for the pelitic lithology association (D–D' in Figure 9), the R_om% values indicate the base of the oil window (about 0.5%) with maximum calculated burials of ~2.5 km. Despite samples belonging to different lithology associations, they derive almost from the base

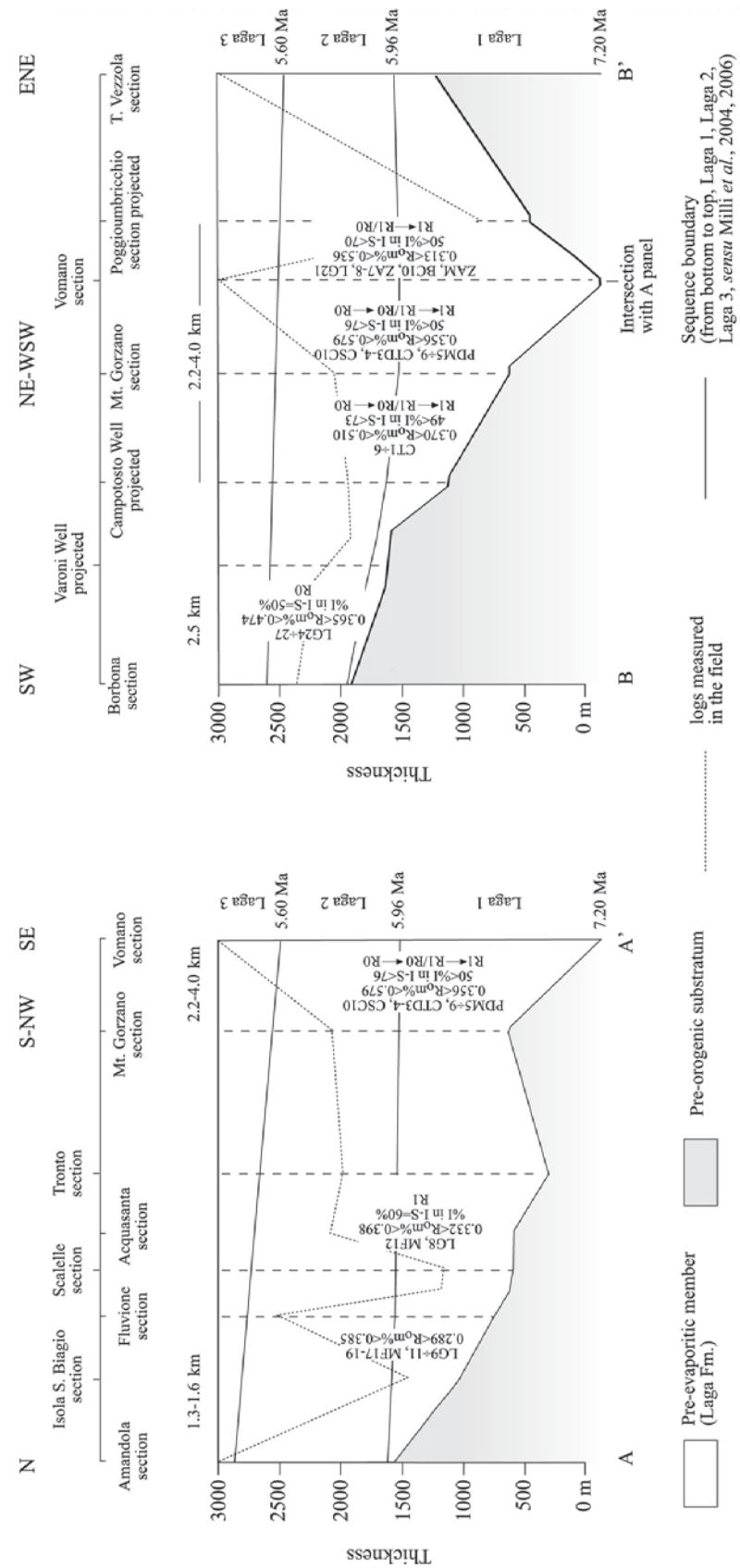

Figure 8. Correlation panels of measured stratigraphic logs across the Laga Basin (after Milli *et al.*, 2006, redrawn and modified) with a summary of selected organic and inorganic thermal parameters and derived burial values as discussed in the text. The Laga Fm. is subdivided into three stratigraphic sequences (from bottom to top named Laga 1, 2 and 3). Localities reported on top indicate locations of logs measured in the field. Traces are shown in Figure 1.

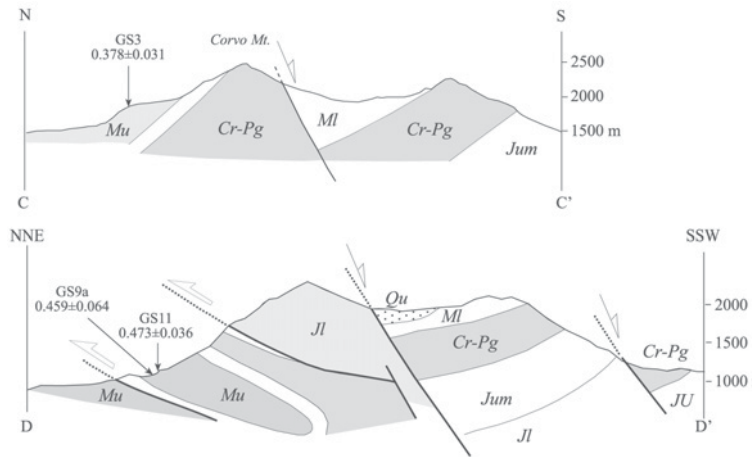

Figure 9. Cross-sections showing the structural setting of the Gran Sasso thrust belt and R_om% samples (see Figure 1 for locations of the C–C' and D–D' cross-sections). Observe the decrease in shortening from the eastern to the western part of the range (redrawn and modified from Ghisetti and Vezzani, 1986, D'Agostino *et al.*, 1998; D'Agostino and Corrado, 1999). Legend: Jl = Lower Jurassic; Jum = Upper–Middle Jurassic; Cr–Pg = Cretaceous–Paleogene; Ml = Lower Miocene; Mu = Upper Miocene (comprising pelitic lithology association); Qu = Quaternary.

of the Laga Fm. and from different structural local settings shown in Figure 9. Sample GS3 belongs to the Laga Fm., which probably never experienced any tectonic loading, while GS11 and GS9a samples are from the nucleus of an overturned syncline which represents the footwall of the Corno Grande thrust sheet. This implies that the Gran Sasso front loses displacement moving from the East to the West as already shown by D'Agostino and Corrado (1999) and Bigi and Casero (2006).

Small values for the Montagna dei Fiori pre-orogenic succession are indicative of scarce syn-orogenic sedimentary burial mainly represented by the preserved Meso-cenozoic pre-orogenic succession itself, in general agreement with fluid inclusion data from the base of the Montagna dei Fiori pre-orogenic succession (Calcare massiccio Fm.). In this unit, homogenization temperatures (Th) are between 70 and 90ºC due to the maximum sedimentary burial which occurred in Middle Miocene times and between 110 and 130ºC due to both hot fluid circulation and sedimentary burial in Upper Miocene times (Ronchi *et al.*, 2003).

Further regional studies based on apatite fission tracks and R_om% on the Laga Basin were recently performed (Calamita *et al.*, 1994; Rusciadelli *et al.*, 2005). They suggest for the Laga Fm. to the west of the Montagnone-Montagna dei Fiori alignment, maximum paleotemperatures ranging between 50 and 110ºC, in agreement with those proposed in the present study. Nevertheless these maximum paleotemperatures are interpreted as the effect of a ubiquitous and homogeneous tectonic loading due to the emplacement of allochthonous units (Rusciadelli *et al.* 2005) or thick sedimentary units, now eroded (Scisciani and Montefalcone, 2005). On the other hand, in our hypothesis, variable sedimentary burial due to the Lower Messinian deposits explains our results, except where local anomalies are recorded at the footwall of regional thrust sheets.

This discrepancy in interpretation is probably due to the generalization of the results obtained from a limited paleotemperature dataset and to the underestimation of the contribution of sedimentary burial to the thermal evolution of the area.

CONCLUSIONS

Mineralogical and organic matter data allowed us to define the thermal evolution of the syn-orogenic deposits and their pre-orogenic substratum in the Laga Basin. A depth-dependent feature is recognized for vitrinite reflectance and I-S. Higher R_om% values and percentages of illite layers in I-S are found in the basin depocenter and at the footwall of the main carbonate thrust sheets. Lower R_om% and I-S values are found in less subsided sectors surrounding the depocenter.

Mixed-layer clay minerals and R_om% are directly related to the burial history of the Laga Basin showing diagenetic conditions. On the contrary, KI values indicate more evolved stages of thermal maturity when compared to organic and other inorganic thermal parameters. These data mainly refer to detrital 10 Å phases, either metamorphic or sedimentary, associated with the uplift of the Alpine-Apennines chain. Thus, KI data cannot be used for the reconstruction of the thermal history of the Laga Basin but do provide information on provenance and thermal conditions of the source rock.

Maximum temperatures calculated from authigenic phases and vitrinite reflectance are <100–110ºC throughout the basin. The acquired thermal maturity of the Laga Fm. is mainly due to sedimentary burial not exceeding 4.0 km in the basin depocenter. A progressive

decrease in thickness to ~1.5 km towards the North reflects the articulated basin physiography in Lower Messinian times. Slightly higher levels of diagenesis are recorded at the footwall of regional thrust sheets.

ACKNOWLEDGMENTS

We are grateful to V. Cantarelli for performing most of the laboratory preparation and re-organizing the database. S. Bigi, P. Casero, N. D'Agostino, S. Milli, M. Moscatelli, O. Stanzione and R. Tyson are kindly acknowledged for stimulating discussions and their help in the field. D.D. Eberl is warmly acknowledged for reviewing the original version of the paper. The organic matter analyses were carried out at the University of Newcastle upon Tyne and XRD analyses at the University of Roma Tre: R. Tyson and C. Giampaolo are acknowledged for the use of facilities. The manuscript was greatly improved by the comments of P. Árkai, A.C. Cook and Associate Editor B. Lanson.

REFERENCES

Allen, P.A. and Allen, R.R. (1993) *Basin Analysis Principles and Applications*. Blackwell, Oxford, UK, 451 pp.

Árkai, P. (2002) Phyllosilicates in very low-grade metamorphism: transformation to micas. Pp. 463–478 in: *Micas: Crystal Chemistry and Metamorphic Petrology* (A. Mottana, F.P. Sassi, J.B. Thompson and S. Guggenheim, editors). Reviews in Mineralogy & Geochemistry **46**, Mineralogical Society of America, Washington, D.C.

Artoni, A. (2003) Messinian events within the tectono-stratigraphic evolution of the Southern Laga Basin (Central Apennines, Italy). *Bollettino della Società Geologica Italiana*, **122**, 447–465.

Barker, C. (1996) *Thermal Modeling of Petroleum Generation: Theory and Applications*. Elsevier, Amsterdam, 512 pp.

Barker, C.E. (1989) Temperature and time in thermal maturation of sedimentary organic matter. Pp. 75–98 in: *Thermal History of Sedimentary Basins* (N.D. Naeser and T.H. McCulloh, editors). Springer-Verlag, New York.

Barker, C.E. and Pawlewicz, M.J. (1994) Calculation of vitrinite reflectance from thermal histories and peak temperatures. A comparison of methods. Pp. 216–229 in: *Vitrinite Reflectance as a Maturity Parameter: Applications and Limitations* (P.K. Mukhopadhyay and W.G. Dow, editors). ACS Symposium Series, **570**, American Chemical Society.

Bigi, S. and Casero, P. (2006) Deep geometry of Laga basin (Central Apennines, Italy). *Geophysical Research Abstracts*, **8**, 06071.

Bigi, S., Casero, P., Corrado, S., Milli, S., Moscatelli, M. and Stanzione, O. (2006) Geometric framework and thermal history of the Laga basin: constraints for integrated basin analysis. *Geophysical Research Abstracts*, **8**, 08484.

Borrego, A.G., Araujo, C.V., Balke, A., Cardott, B., Cook, A.C., David, P., Flores, D., Hámor-Vidó, M., Hiltmann, W., Kalkreuth, W., Koch, J., Kommeren, C.J., Kusc, J., Ligouis, B., Marques, M., Mendonça Filho, J.G., Misz, M., Oliveira, L., Pickel, W., Reimer, K., Ranasinghe, P., Suárez-Ruiz, I. and Vieth, A. (2006) Influence of particle and surface quality on the vitrinite reflectance of dispersed organic matter: comparative exercise using data from the qualifying system for reflectance analysis working group of ICCP. *International Journal of Coal Geology*, **68**, 151–170.

Bucher, K. and Frey, M. (1994) *Petrogenesis of Metamorphic Rocks*. Springer-Verlag, Berlin, 318 pp.

Calamita, F., Cello, G., Deiana, G. and Paltrinieri, W. (1994) Structural styles, chronology rates of deformation, and time-space relationships in the Umbria-Marche thrust system (central Apennines, Italy). *Tectonics*, **13**, 873–881.

Carosi, R., Leoni, L., Montomoli, C. and Sartori, F. (2003) Very low-grade metamorphism in the Tuscan Nappe, Northern Apennines, Italy: relationships between deformation and metamorphic indicators in the La Spezia mega-fold. *Schweizerische Mineralogische und Petrographische Mitteilungen*, **83**, 15–32.

Centamore, E., Cantalamessa, G., Micarelli, A., Potetti, M., Berti, D., Bigi, S., Morelli, C. and Ridolfi, M. (1991) Stratigrafia e analisi di facies dei depositi del Miocene e del Pliocene inferiore dell'avanfossa marchigiano-abruzzese e delle zone limitrofe. *Studi Geologici Camerti*, **1991/2**, 125–131.

Corda, L. and Morelli, C. (1996) Compositional evolution of the Laga and Cellino sandstones (Messinian-Lower Pliocene, Adriatic foredeep). *Bollettino della Società Geologica Italiana*, **115**, 423–437.

D'Agostino, N. and Corrado, S. (1999) Differential erosion along a mountain front: geomorphological and organic matter thermal analyses in the Gran Sasso Range (Central Italy). *International workshop on: 'Large scale vertical movements and related gravitational processes'*. Abstract volume, p. 51, Camerino, Rome.

D'Agostino, N., Chamot-Rooke, N., Funiciello, R., Jolivet, L. and Speranza, F. (1998) The role of pre-existing thrust faults and topography on the styles of extension in the Gran Sasso range (central Italy). *Tectonophysics*, **292**, 229–254.

Essene, E.J. and Peacor, D.R. (1995) Clay mineral thermometry – a critical perspective. *Clays and Clay Minerals*, **43**, 540–553.

Gharrabi, M., Velde, B. and Sagon, J.-P. (1998) The transformation of illite to muscovite in pelitic rocks: constraints from X-ray diffraction. *Clays and Clay Minerals*, **46**, 79–88.

Ghisetti, F. and Vezzani, L. (1986) Assetto geometrico ed evoluzione strutturale della catena del Gran Sasso tra Vado di Siella e Vado di Corno. *Bollettino della Società Geologica Italiana*, **105**, 131–171.

Heling, D. and Teichmüller, M. (1974) Die Grenze Montmorillonite/Mixed Layer-Minerale und ihre Beziehung zur Inkohlung in der Grauen Schichtenfolge des Oligozäns im Oberrheingraben. *Fortschritte in der Geologie von Rheinland und Westfalen*, **24**, 113–128.

Hillier, S. (1993) Origin, diagenesis, and mineralogy of chlorite minerals in Devonian lacustrine mudrocks, Orcadian Basin, Scotland. *Clays and Clay Minerals*, **41**, 240–259.

Hoffman, J. and Hower, J. (1979) Clay mineral assemblages as low grade metamorphic geothermometers: applications to the thrust faulted disturbed belt of Montana, USA. Pp. 55–79 in: *Aspect of Diagenesis* (P.A. Scholle and P.R. Schluger, editors). Special Publication **26**, The Society of Economic Paleontologists and Mineralogists, Tulsa, Oklahoma.

Hower, J., Eslinger, E.V., Hower, M.E. and Perry, E.A. (1976) Mechanism of burial metamorphism of argillaceous sediment – mineralogical and chemical evidence. *Geological Society of America Bulletin*, **87**, 725–737.

Kisch, H.J. (1991) Illite crystallinity: recommendations on sample preparation, X-ray diffraction settings, and interlaboratory samples. *Journal of Metamorphic Geology*, **9**, 665–670.

Kisch, H.J., Árkai, P. and Brime, C. (2004) On the calibration of the illite Kübler index (illite 'crystallinity'). *Schweizerische Mineralogische und Petrographische Mitteilungen*, **84**, 323–331.

Lanson, B. (1997) Decomposition of experimental X-ray

diffraction patterns (profile fitting): a convenient way to study clay minerals. *Clays and Clay Minerals*, **45**, 132–146.

Leoni, L. (2001) New standardized illite crystallinity data from low – to very-low grade metamorphic rocks (Northern Apennines, Italy). *European Journal of Mineralogy*, **13**, 1109–1118.

Leoni, L., Marroni, M., Sartori, F. and Tamponi, M. (1996) Metamorphic grade in metapelites of the Internal Liguride Units (Northern Apennines, Italy). *European Journal of Mineralogy*, **8**, 35–50.

Manzi, V., Lugli, S., Ricci Lucchi, F. and Roveri, M. (2005) Deep-water clastic evaporites deposition in the Messinian Adriatic foredeep (northern Apennines, Italy): did the Mediterranean ever dry out? *Sedimentology*, **52**, 875–902.

Merriman, R.J. and Frey, M. (1999) Patterns of very low-grade metamorphism in metapelitic rocks. Pp. 61–107 in: *Low-grade Metamorphism* (M. Frey and D. Robinson, editors). Blackwell, Oxford, UK.

Merriman, R.J. and Kemp, S.J. (1996) Clay minerals and sedimentary basin maturity. *Mineralogical Society Bulletin*, **111**, 7–8.

Milli, S., Moscatelli, M., Stanzione, O., Gennari, G. and Marini, M. (2004) Sedimentology and physical stratigraphy of the pre-gypsum arenites deposits of the Laga formation. *32nd International Geological Congress*, Abstract volume session G21.05, Firenze, Italy.

Milli, S., Moscatelli, M., Stanzione, O., Falcini, F. and Bigi, S. (2006) *The Messinian Laga Formation: facies, geometries, stratigraphic architecture and structural style of a confined turbidite basin (Central Appennines, Italy). Excursion Guidebook.* Università degli Studi 'La Sapienza', Rome, 55 pp.

Moore, D.M. and Reynolds, R.C. Jr. (1997) *X-ray Diffraction and the Identification and Analysis of Clay Minerals*. Oxford University Press, New York, 378 pp.

Moscatelli, M., Milli, S., Stanzione, O., Marini, M., Gennari, G. and Vallone, R. (2004) I depositi torbiditici del Messiniano inferiore dell'Appennino Centrale: bacino del Salto-Tagliacozzo e della Laga (Lazio, Abruzzo, Marche). *2nd GeoSed Meeting, Post-congress Field Trip Guidebook*, 65, Rome.

Parotto, M. and Praturlon, A. (1975) Geological summary of the Central Apennines. Pp. 257–311 in: *Structural Model of Italy* (L. Ogniben, M. Parotto, and A. Praturlon, editors). Quaderni della Ricerca Scientifica **90**, C.N.R, Rome.

Pollastro, R.M. (1993) Consideration and applications of the illite/smectite geothermometer in hydrocarbon-bearing rocks of Miocene to Mississipian age**.** *Clays and Clay Minerals*, **41**, 119–133**.**

Pollastro, R. and Barker, C.E. (1986) Application of clay mineral, vitrinite reflectance, and fluid inclusion studies to the thermal and burial history of the Pinedale Anticline, Green River Basin, Wyoming. Pp. 73–83 in: *Roles of Organic Matter in Sediment Diagenesis* (D.L. Gautier, editor). Special Publication **38**, The Society of Economic Paleontologists and Mineralogists, Tulsa, Oklahoma.

Price, L.C. (1983) Geologic time as a parameter in organic metamorphism and vitrinite reflectance as an absolute paleogeothermometer. *Journal of Petroleum Geology*, **6**, 5–38.

Price, L.C. and Barker, C.E. (1985) Suppression of vitrinite reflectance in amorphous rich kerogen – a major unrecognized problem. *Journal of Petroleum Geology*, **8**, 59–84.

Ronchi, P., Casaglia, F. and Ceriani, A. (2003) The multiphase dolomitization of the Liassic Calcare Massiccio e Corniola successions (Montagna dei Fiori, Northern Apennines, Italy). *Bollettino della Società Geologica Italiana*, **122**, 157–172.

Rusciadelli, G., Viandante, M.G., Calamita, F. and Cook, A.C. (2005) Burial-exhumation history of the central Apennines (Italy), from the foreland to the chain building: thermochronological and geological data. *Terra Nova*, **17**, 560–572.

Scisciani, V. and Montefalcone, R. (2005) Evoluzione neogenico-quaternaria del fronte della catena centro-appenninica: vincoli dal bilanciamento sequenziale di una sezione geologica regionale. *Bollettino della Società Geologica Italiana*, **124**, 579–599.

Środoń, J. (1999) Nature of mixed-layer clays and mechanisms of their formation and alteration. *Annual Review of Earth and Planetary Sciences*, **27**, 19–53.

Stach, E., Mackowsky, M.-Th., Teichmüller, M., Taylor, G.H., Chandra, D. and Teichmüller, R. (1982) *Stach's Textbook of Coal Petrology*. Gebruder Borntraeger, Berlin, 535 pp.

Teichmüller, M. (1987) Organic material and very low-grade metamorphism. Pp. 114–161 in: *Low Temperature Metamorphism* (M. Frey, editor). Blackie, Glasgow and London.

Valloni, R., Cipriani, N. and Morelli, C. (2002) Petrostratigraphic record of the Apennine foredeep basins, Italy. *Bollettino della Società Geologica Italiana*, spec. vol. **1**, 455–465.

Wang, H., Stern, W.B. and Frey, M. (1995) Deconvolution of the X-ray 'Illite' 10-Å complex: a case study of the Helvetic sediments from eastern Switzerland. *Schweizerische Mineralogische und Petrographische Mitteilungen*, **75**, 187–199.

Wang, H., Frey, M. and Stern, W.B. (1996) Diagenesis and metamorphism of clay minerals in the Helvetic Alps of Eastern Switzerland. *Clays and Clay Minerals*, **44**, 96–112.

Warr, L.N. and Rice, A.H.N. (1994) Interlaboratory standardization and calibration of clay mineral crystallinity and crystallite size data. *Journal of Metamorphic Geology*, **12**, 141–152.

Weaver, C.E. and Broekstra, B.R. (1984) Illite-mica. Pp. 67–97 in: *Shale-slate Metamorphism in the Southern Appalachians* (C.E. Weaver, editor). Developments in Petrology, **10**, Elsevier, New York.

Zattin, M., Picotti, V. and Zuffa, G.G. (2002) Fission-track reconstruction of the front of the Northern Apennine thrust wedge and overlying Ligurian Unit. *American Journal of Science*, **302**, 346–379.

(*Received 15 January 2007; revised 20 June 2007; Ms. 1246; A.E. Bruno Lanson*)